10-2014

A Regression Approach for Estimation of Anthropogenic Heat Flux Based on a Bottom-Up Air Pollutant Emission Database

Sang-Hyun Lee
Kongju National University

Stuart A. McKeen
NOAA Earth System Research Laboratory

David J. Sailor
Portland State University

Citation Details

Lee, S. H., McKeen, S. A., & Sailor, D. J. (2014). A regression approach for estimation of anthropogenic heat flux based on a bottom-up air pollutant emission database. Atmospheric Environment, 95, 629-633.

Atmospheric Environment 95 (2014) 629–633

Contents lists available at ScienceDirect

Atmospheric Environment

journal homepage: www.elsevier.com/locate/atmosenv

Technical note

A regression approach for estimation of anthropogenic heat flux based on a bottom-up air pollutant emission database

Sang-Hyun Lee [a,*], Stuart A. McKeen [b], David J. Sailor [c]

[a] Department of Atmospheric Science, Kongju National University, Gongju 314-701, South Korea
[b] Chemical Sciences Division, NOAA Earth System Research Laboratory and University of Colorado/CIRES, Boulder, CO 80305, USA
[c] Department of Mechanical and Materials Engineering, Portland State University, Portland, OR 97207, USA

HIGHLIGHTS

- A new methodology for anthropogenic heat flux (AHF) estimation is suggested.
- The AHF over the entire US regions is estimated at 4-km and 1-h resolution.
- The gridded AHF dataset is publicly available via a ftp site.

ARTICLE INFO

Article history:
Received 2 February 2014
Received in revised form
27 June 2014
Accepted 2 July 2014
Available online 3 July 2014

Keywords:
Anthropogenic heat
Energy balance
Urban heat islands
Urban modeling
Waste heat

ABSTRACT

A statistical regression method is presented for estimating hourly anthropogenic heat flux (AHF) using an anthropogenic pollutant emission inventory for use in mesoscale meteorological and air-quality modeling. Based on bottom-up AHF estimated from detailed energy consumption data and anthropogenic pollutant emissions of carbon monoxide (CO) and nitrogen oxides (NO_x) in the US National Emission Inventory year 2005 (NEI-2005), a robust regression relation between the AHF and the pollutant emissions is obtained for Houston. This relation is a combination of two power functions ($Y = aX^b$) relating CO and NO_x emissions to AHF, giving a determinant coefficient (R^2) of 0.72. The AHF for Houston derived from the regression relation has high temporal ($R = 0.91$) and spatial ($R = 0.83$) correlations with the bottom-up AHF. Hourly AHF for the whole US in summer is estimated by applying the regression relation to the NEI-2005 summer pollutant emissions with a high spatial resolution of 4-km. The summer daily mean AHF range 10–40 W m^{-2} on a 4 × 4 km^2 grid scale with maximum heat fluxes of 50–140 W m^{-2} for major US cities. The AHFs derived from the regression relations between the bottom-up AHF and either CO or NO_x emissions show a small difference of less than 5% (4.7 W m^{-2}) in city-scale daily mean AHF, and similar R^2 statistics, compared to results from their combination. Thus, emissions of either species can be used to estimate AHF in the US cities. An hourly AHF inventory at 4 × 4 km^2 resolution over the entire US based on the combined regression is derived and made publicly available for use in mesoscale numerical modeling.

1. Introduction

Anthropogenic energy consumption generated from fossil fuels (e.g. coal, petroleum, natural gas) results in dissipation to heat on short timescales, which is released as sensible and/or latent heat to the atmosphere (Sailor, 2011). For many cities in the world, diurnal anthropogenic heat flux (AHF) ranges approximately 10–100 W m^{-2} on a city scale and larger AHFs are found in urban centers exceeding 100–400 W m^{-2} at a specific location in different seasons (e.g. Ichinose et al., 1999; Kłysik, 1996; Sailor and Lu, 2004; Pigeon et al., 2007; Heiple and Sailor, 2008; Lee et al., 2009; Smith et al., 2009; Iamarino et al., 2012). In general, AHF is larger in winter than in summer and larger during daytime than at night according to temporal variations of human activity (e.g. Lee et al., 2009; Sailor and Lu, 2004).

Atmospheric influences of urban AHF on meteorology/climate have been widely investigated from local to regional/global scales using numerical simulations (e.g. Block et al., 2004; Fan and Sailor, 2005; Makar et al., 2006; Ohashi et al., 2007; Chen et al., 2009; Flanner, 2009). Previous studies found that AHF could increase

* Corresponding author.
E-mail address: sanghyun@kongju.ac.kr (S.-H. Lee).

http://dx.doi.org/10.1016/j.atmosenv.2014.07.009
1352-2310/

near-surface air temperature by 1–3 °C on average under different meteorological and geographical conditions and made urban atmospheric boundary layer (ABL) more unstable, leading to urban-breeze circulations. The atmospheric influences are found to be more important during nighttime and in winter due to less turbulent mixing in the ABL. Furthermore, urban AHF may modify gaseous/aerosol chemical reactions, anthropogenic/biogenic pollutant emissions and their atmospheric residence time (Crutzen, 2004; Flanner, 2009). Recently, Ryu et al. (2013) reported that the urban AHF can enhance urban ozone concentration by 2–5 ppb during a diurnal cycle in a megacity (Seoul in South Korea) as a result of complicated interactions between meteorology and in-situ photochemistry.

The AHF data required for atmospheric and environmental numerical modeling are generally estimated by bottom-up or top-down approaches based on energy consumption data available for a city. The main anthropogenic sources include the building sector (electricity, heating/cooling energy use, etc) and the vehicle sector. For some cities, however, emissions from the industrial sector are also important. The bottom-up approach uses building-level energy consumption data within a city with high temporal resolution (~1 h) calculated from energy consumption monitoring (or modeling) of representative buildings and geographical information (e.g. Ichinose et al., 1999; Kikegawa et al., 2006; Heiple and Sailor, 2008), while the top-down approach uses city-scale energy consumption data and climatological (statistical) temporal (hourly) variations (e.g. Sailor and Lu, 2004). Therefore, the AHF in the bottom-up approach is estimated in the aggregate of building-level energy consumption to a grid-cell size of interest, while the AHF in the top-down approach is calculated by applying gridded spatial surrogates (e.g. population density, road area) to the city-scale energy consumption. The bottom-up estimation can give more accurate spatial and temporal distributions within a city than the top-down estimation by virtue of the high spatial and temporal resolution of energy consumption data, but they use energy-related inventories for AHF estimation. Here, we develop an AHF estimation method based on a statistical regression relationship between AHF and anthropogenic emissions of carbon monoxide (CO) and nitrogen oxides ($NO_x = NO + NO_2$), and discuss the AHF for the whole US in summer resulting from the proposed relationship. CO and NO_x are produced as a consequence of human activity (e.g. fossil fuel combustion, vehicles) and their emissions are rigorously compiled within a national inventory by the US EPA based on observed emission factors and activity data provided by state and local government agencies. Since the activity data in the emissions inventory is correlated with energy consumption data used for AHF estimations, anthropogenic heat and air pollutant emissions are expected to have significant similarity in spatial and temporal distribution.

The manuscript is presented as follows. Section 2 describes a statistical regression method for AHF estimation using bottom-up anthropogenic heat and air pollutant emissions. The summer AHF for the whole US estimated by the regression method is presented in Section 3, and summary and conclusions follow in Section 4.

2. Development of a regression method for anthropogenic heat fluxes

The anthropogenic heat and pollutant emissions are estimated based on quite similar emission inventories, but different conversion factors are applied for anthropogenic heat and air pollutant emissions. This fact leads to finding a regression relation between the two different anthropogenic emissions. The present study uses the AHF for Houston, Texas, US in August estimated from a combination of intensive bottom-up energy consumption analysis by Heiple and Sailor (2008) for the building sector and general top-down inventory-based analysis by Sailor and Lu (2004) for the vehicle and industry sectors, hereafter, bottom-up AHF. CO and NO_x emissions in summer are derived from the US Environmental Protection Agency (EPA) National Emission Inventory year 2005 (NEI-2005) (US EPA, 2010) using a bottom-up approach (ftp://aftp.fsl.noaa.gov/divisions/taq/emissions_data_2005/).

Both heat and pollutant emissions were aggregated to hourly and 4-km gridded data for regression analysis. The NEI-2005 inventory includes area, point, mobile-onroad, mobile-nonroad sectors. The area and point emissions were processed based on NEI-2002 version 3 emissions (US EPA, 2008) and updated Continuous Emissions Monitoring System (CEMS) for August 2006. The mobile emissions were estimated from the National Mobile Inventory Model (NMIM) for July 2006 using the MOBILE6.2 and NONROAD2005 models (US EPA, 2005). Seven primary atmospheric pollutants' emissions (CO, NO_x, SO_2, NH_3, $PM_{2.5}$, PM_{10}, VOC) are included in the NEI-2005 emissions for the whole US. Among them, CO and NO_x emissions were selected for statistical regression analysis in this study because they are emitted from diverse anthropogenic sources in urban areas (e.g. point, mobile, and area sources) and their production is closely related to combustion processes in human activity, thus leading to simultaneous anthropogenic heat emissions. CO is produced from the processes of incomplete burning of carbon-containing fossil fuels (e.g. coal, gas, oil) in on-road and nonroad vehicles and engines (e.g. cars, trucks, aircraft, marine vessels, farm/construction equipment), industrial/commercial facilities (e.g. power plants, department stores), residential heating (e.g. stoves, boilers) and cooking, while NO_x is also produced as a consequence of combustion at high temperature, thus major anthropogenic sources are electricity-generating power plants, motor vehicles, industrial facilities, and residential fuel-burning appliances. For the regression analysis below only CO and NO_x emissions from the on-road and nonroad vehicle sectors and area type sources (e.g. industrial and institutional boilers, and residential heating) are considered. Point sources for both these species are not included in the regression since they are typically located outside urban settings.

Fig. 1 shows the scatter plots between the AHF and NEI-2005 emissions of CO and NO_x for Houston. First we removed grid cells that are significant outliers due to the influence of point sources and uncertainties on both the AHF and pollutant dataset using filtering conditions as follow: daily mean AHF > 1 W m^{-2}; daily mean CO emission < 70 kg km^{-2} h^{-1}; daily mean NO_x emission < 10 kg km^{-2} h^{-1}. After filtering off the outliers, hourly data on 154 grid cells (2464 km^2) are compared for the regression analysis. It shows that both anthropogenic CO and NO_x surface fluxes (kg km^{-2} h^{-1}) are well correlated with the AHF (W m^{-2}) as was expected. For each CO and NO_x emission, a power regression function is found the AHF fitting well as follows:

$$Y_{AHF}^{CO} = 2.55X_{CO}^{0.64},$$

$$Y_{AHF}^{NO_x} = 8.32X_{NO_x}^{0.69},$$

where X_{CO}, X_{NO_x} are hourly anthropogenic CO and NO_x (as NO_2 equivalent amount) emissions in kg km^{-2} h^{-1} and Y_{AHF}^{CO}, $Y_{AHF}^{NO_x}$ are the estimates of AHF in W m^{-2}. Approximately 70% of variance in the bottom-up AHF estimation is explained by the regression of CO ($R^2 = 0.717$) and NO_x ($R^2 = 0.707$) emissions, where R^2 is the coefficient of determination in the regression fit. The AHF for Houston resulting from the regression relation has high temporal ($R = 0.90$ for CO and $R = 0.93$ for NO_x) and spatial ($R = 0.84$ for CO and $R = 0.80$ for NO_x) correlations with the bottom-up AHF.

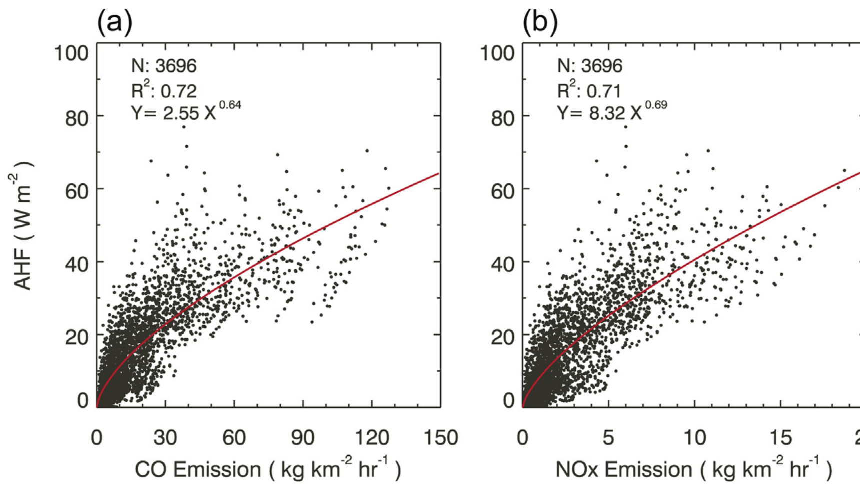

Fig. 1. Scatter plots between bottom-up anthropogenic heat flux and NEI-2005 anthropogenic pollutant emissions for Houston, US in summer: (a) CO and (b) NO_x. The bottom-up AHF is estimated by a combination of Heiple and Sailor (2008) and Sailor and Lu (2004).

Uncertainties in either CO or NO_x emission can influence the AHF estimation. Therefore, to minimize the influence, the AHF regression relation is obtained by the combination of the two regression relations as follows:

$$Y_{\mathrm{AHF}} = \alpha Y_{\mathrm{AHF}}^{\mathrm{CO}} + (1-\alpha) Y_{\mathrm{AHF}}^{\mathrm{NO}_x}.$$

Here, a weight factor $\alpha = 0.5$ is assigned on the assumption that each relation has same magnitude of errors. The resultant mean regression relation leads to the determinant coefficient (R^2) of 0.723 and temporal and spatial correlation coefficients of $R = 0.91$ and $R = 0.83$, respectively.

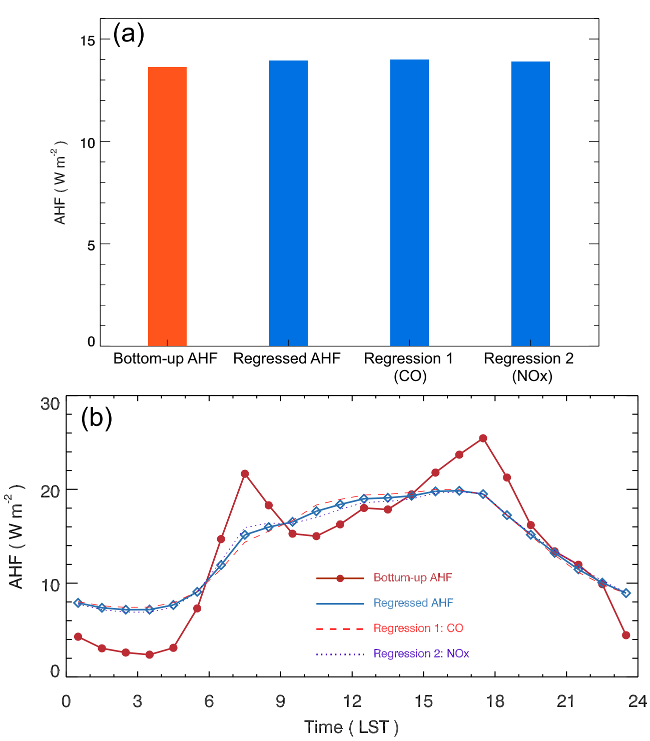

Fig. 2. Comparison of bottom-up anthropogenic heat flux for Houston with anthropogenic heat fluxes resulting from regression relations from CO and NO_x emissions: (a) city-scale AHF in W m^{-2} and (b) AHF temporal variations.

Fig. 2 compares the bottom-up AHF and estimates using the regression relations in terms of city-scale mean magnitude and temporal variation. The city-scale mean AHF (13.9 W m^{-2}) estimated by the mean regression relation compares well to the bottom-up AHF (13.6 W m^{-2}) with a difference of 2.2%. The AHF estimate from each regression relation using CO and NO_x emissions is slightly greater than the bottom-up AHF, but has little difference (less than 1%) between each other (Fig. 2a). The diurnal profile in the bottom-up AHF shows that energy consumption in Houston is large during the daytime with salient peaks in the morning and evening mainly due to the increase of traffic during rush hours (Sailor and Lu, 2004). Meanwhile, the AHF estimate from the regression relation compares well with the bottom-up AHF in diurnal variation ($R = 0.91$), with the largest relative difference (>40%) found at night between 12:00 am and 5:00 am LST. The difference of the AHF temporal profiles is largely attributed to the hourly profiles of CO and NO_x emissions for the vehicle sector in Houston. They have smoothed peaks in morning and evening rush hours and a higher emission fraction at the nighttime period compared to the top-down hourly profile of mobile sector used in the AHF estimation (see Fig. 2 in Sailor and Lu, 2004). Spatial distributions of the AHFs are well correlated during a diurnal cycle with high spatial correlation coefficient (R) values ranging 0.77–0.86. The minimum R value of 0.77 is found around 3–4 LST. Note that the regression estimate of AHF is derived from spatial and temporal characteristics of the bottom-up pollutant emissions, therefore, the use of the regression estimate for AHF provides consistent diurnal profiles between anthropogenic heat and pollutant emissions for air quality modeling.

3. Application of regression method to AHF estimation for the whole US

The regression relation established in Section 2 is easily applied for estimation of AHF with the anthropogenic bottom-up CO and NO_x emissions available in the NEI-2005 inventory. Fig. 3 presents summer daily mean AHF for the whole US resulting from the application of the mean regression relation derived for Houston to the NEI-2005 emissions. The daily mean AHF is distinctively high for major US cities, ranging 10–40 W m^{-2} on a grid scale (4×4 km^2). In addition, the AHFs on roads (local roads and intercity highways) are also clearly seen with a magnitude of 2–8 W m^{-2}. The temporal profile of the AHF at each grid cell is inherited from the NEI-2005 emissions.

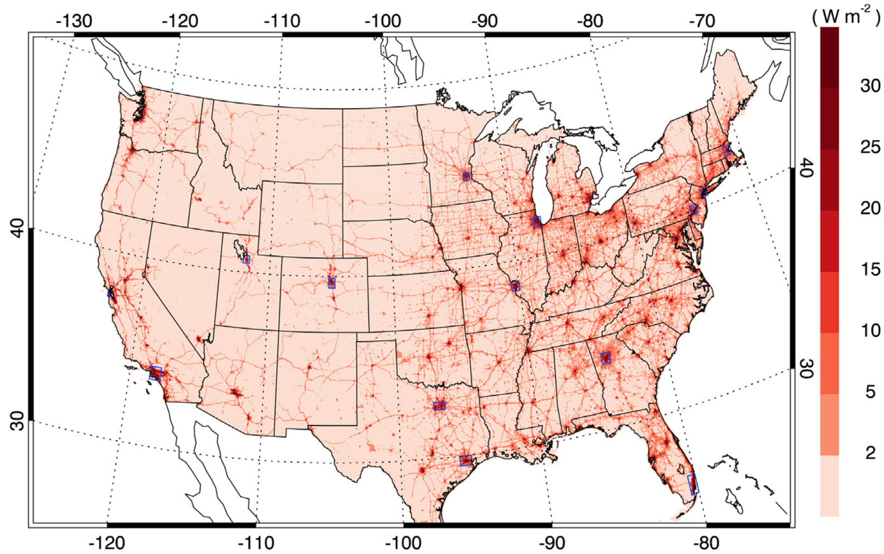

Fig. 3. Spatial distribution of summer daily mean anthropogenic heat fluxes derived from the mean regression relation.

Fig. 4 compares the city-scale summer daily mean AHF estimates resulting from different regression relations for 14 US cities, and Table 1 presents geographical boundary for city-scale AHF analysis and mean/maximum AHF for each city. The city-scale daily mean AHF ranges 10–30 W m^{-2} for the US cities in summer, a spatial standard deviation of daily mean AHF within a city ranges 10–20 W m^{-2} (Fig. 4). Maximum daily mean AHF within each city ranges 50–140 W m^{-2} on a grid scale (Table 1). The difference in daily mean AHF estimates resulting from CO and NO_x regression relations is at most 4.7 W m^{-2} for Chicago, and their fractional difference normalized by mean regression estimate are within 5% for all the cities (Fig. 4).

In deriving Figs. 3 and 4, we have assumed that the same regression determined for Houston applies to all other US cities and regions. An extension of this work to other cities with high quality, bottom-up AHF estimates is needed to confirm this assumption. The regression relationship between AHF and CO/NO_x emissions for a specific urban center may depend on factors this study is unable to consider. This includes a dependence on specific climate zone, urban/suburban land-use mix, building heat and cooling efficiencies, etc.

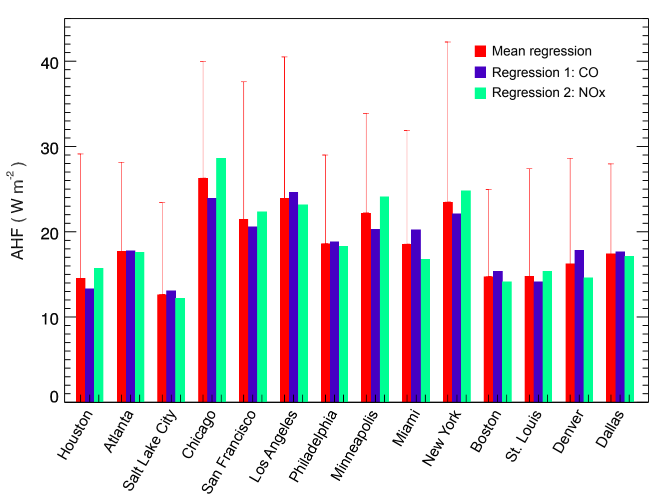

Fig. 4. Comparison of daily mean anthropogenic heat fluxes for 14 US cities estimated from regression relations with CO and NO_x emissions. Vertical bar represents a spatial standard deviation of the AHF in each city. Each city's boundary definition is given in Fig. 3 (box) and Table 1.

4. Summary and conclusions

Here, we developed a simple regression method that estimates AHF using bottom-up anthropogenic pollutant emissions (CO and NO_x) data for Houston. The AHF estimated from the derived regression relation shows good spatial and temporal agreements with the bottom-up AHF, explaining about 72% of the variance of

Table 1
City region definition and mean and maximum anthropogenic heat fluxes for 14 US cities in summer. Maximum AHF is found on 4 × 4 km^2 grid cells.

City	Longitude/latitude	Mean AHF (W m^{-2})	Maximum AHF (W m^{-2})
Houston	Lon: −95.8°–−95.0° Lat: 29.5°–30.0°	14.6	144.0
Atlanta	Lon: −84.7°–−84.1° Lat: 33.5°–34.1°	17.7	72.5
Salt Lake City	Lon: −112.2°–−111.7° Lat: 40.5°–40.9°	12.7	45.8
Chicago	Lon: −88.1°–−87.5° Lat: 41.6°–42.1°	26.3	83.1
San Francisco	Lon: −122.6°–−122.3° Lat: 37.6°–37.9°	21.5	59.0
Los Angeles	Lon: −118.5°–−117.7° Lat: 33.6°–34.3°	23.9	114.5
Philadelphia	Lon: −75.4°–−74.9° Lat: 39.8°–40.3°	18.6	51.2
Minneapolis	Lon: −93.5°–−93.0° Lat: 44.7°–45.1°	22.2	81.1
Miami	Lon: −80.5°–−80.0° Lat: 25.5°–26.5°	18.5	68.5
New York	Lon: −74.2°–−73.7° Lat: 40.5°–40.9°	23.5	137.4
Boston	Lon: −71.4°–−70.8° Lat: 42.1°–42.6°	14.7	66.7
St. Louis	Lon: −90.6°–−90.0° Lat: 38.4°–38.9°	14.8	68.6
Denver	Lon: −105.2°–−104.7° Lat: 39.4°–39.9°	16.2	47.5
Dallas	Lon: −97.4°–−96.6° Lat: 32.6°–33.0°	17.4	65.9

the bottom-up AHF. A gridded summer AHF for the whole US is estimated with high spatial (4 km) and temporal (1 h) resolution by applying the regression relation to the US EPA NEI-2005 emission inventory. This gridded AHF data-set is publicly available (ftp://aftp.fsl.noaa.gov/divisions/taq/NEI_heatflux/) for use in mesoscale meteorological and air quality modeling.

The representation of urban effects in mesoscale numerical modeling is achieved by a physical parameterization associated with urban structure factors (e.g. building geometry, dynamic/thermal/radiative properties) (e.g. Lee and Park, 2008) and inclusion of anthropogenic heat emissions in the thermal energy conservation equation as a form of surface sensible heat fluxes (e.g. Fan and Sailor, 2005; Lee and Baik, 2011). High resolution gridded AHF data for many cities has traditionally been estimated by top-down or bottom-up approaches based on city specific available energy consumption data (Sailor, 2011). The regression method proposed in this study provides gridded AHF estimates over the continental US for mesoscale meteorological and environmental modeling without the intensive effort required in traditional bottom-up AHF estimation approaches.

Acknowledgments

The authors acknowledge two anonymous reviewers for their valuable comments. We also thank Dr. Steven Peckham at NOAA/ESRL for his technical assistance. This work was funded by the Korea Meteorological Administration Research and Development Program under Grant CATER 2012-3081. Part of this work (S.A. McKeen) is supported by the US Weather Research Program within NOAA/OAR Office of Weather and Air Quality.

References

Block, A., Keuler, K., Schaller, E., 2004. Impacts of anthropogenic heat on regional climate patterns. Geophys. Res. Lett. 31. L12211, 1–4.
Chen, Y., Jiang, W., Zhang, N., He, X., Zhou, R., 2009. Numerical simulation of the anthropogenic heat effect on urban boundary layer structure. Theor. Appl. Climatol. 97, 123–134.
Crutzen, P.J., 2004. New directions: the growing urban heat and pollution "island" effect—impact on chemistry and climate. Atmos. Environ. 38, 3539–3540.
Fan, H., Sailor, D.J., 2005. Modeling the impacts of anthropogenic heating on the urban climate of Philadelphia: a comparison of implementations in two PBL schemes. Atmos. Environ. 39, 73–84.
Flanner, M.G., 2009. Integrating anthropogenic heat flux with global climate models. Geophys. Res. Lett. 36, L02801. http://dx.doi.org/10.1029/2008GL036465.
Heiple, S., Sailor, D.J., 2008. Using building energy simulation and geospatial modeling techniques to determine high resolution building sector energy consumption profiles. Energy Build. 40, 1426–1436.
Iamarino, M., Beevers, S., Grimmond, C., 2012. High-resolution (space, time) anthropogenic heat emissions: London 1970–2025. Int. J. Climatol. 32, 1754–1767.
Ichinose, T., Shimodozono, K., Hanaki, K., 1999. Impact of anthropogenic heat on urban climate in Tokyo. Atmos. Environ. 33, 3897–3909.
Kikegawa, Y., Genchi, Y., Kondo, H., Hanaki, K., 2006. Impacts of city-block-scale countermeasures against urban heat-island phenomena upon a building's energy-consumption for air-conditioning. Appl. Energy 83, 649–668.
Kłysik, K., 1996. Spatial and seasonal distribution of anthropogenic heat emissions in Lodz, Poland. Atmos. Environ. 30, 3397–3404.
Lee, S.-H., Baik, J.-J., 2011. Evaluation of the vegetated urban canopy model (VUCM) and its impacts on urban boundary layer simulation. Asia-Pac. J. Atmos. Sci. 47, 151–165.
Lee, S.-H., Park, S.-U., 2008. A vegetated urban canopy model for meteorological and environmental modelling. Bound.-Layer Meteorol. 126, 73–102.
Lee, S.-H., Song, C.-K., Baik, J.-J., Park, S.-U., 2009. Estimation of anthropogenic heat emission in the Gyeong-In region of Korea. Theor. Appl. Climatol. 96, 291–303.
Makar, P., Gravel, S., Chirkov, V., Strawbridge, K., Froude, F., Arnold, J., Brook, J., 2006. Heat flux, urban properties, and regional weather. Atmos. Environ. 40, 2750–2766.
Ohashi, Y., Genchi, Y., Kondo, H., Kikegawa, Y., Yoshikado, H., Hirano, Y., 2007. Influence of air-conditioning waste heat on air temperature in Tokyo during summer: numerical experiments using an urban canopy model coupled with a building energy model. J. Appl. Meteorol. Climatol. 46, 66–81.
Pigeon, G., Legain, D., Durand, P., Masson, V., 2007. Anthropogenic heat release in an old European agglomeration (Toulouse, France). Int. J. Climatol. 27, 1969–1981.
Ryu, Y.-H., Baik, J.-J., Lee, S.-H., 2013. Effects of anthropogenic heat on ozone air quality in a megacity. Atmos. Environ. 80, 20–30.
Sailor, D.J., 2011. A review of methods for estimating anthropogenic heat and moisture emissions in the urban environment. Int. J. Climatol. 31, 189–199.
Sailor, D.J., Lu, L., 2004. A top–down methodology for developing diurnal and seasonal anthropogenic heating profiles for urban areas. Atmos. Environ. 38, 2737–2748.
Smith, C., Lindley, S., Levermore, G., 2009. Estimating spatial and temporal patterns of urban anthropogenic heat fluxes for UK cities: the case of Manchester. Theor. Appl. Climatol. 98, 19–35.
U.S. Environmental Protection Agency (EPA), 2005. EPA's National Mobile Inventory Model (NMIM), a Consolidated Emissions Modeling System for MOBILE6 and NONROAD. EPA420-R-05-024, 24 pp., Washington, D.C. http://www.epa.gov/otaq/models/nmim/420r05024.pdf.
U.S. Environmental Protection Agency (EPA), 2008. Technical Support Document: Preparation of Emissions Inventories for the 2002-based Platform, Version 3, Criteria Air Pollutants, 77 pp., Office of Air Quality Planning and Standards, Air Quality Assessment Division. http://www.epa.gov/ttn/scram/reports/Emissions%20TSD%20Vol1_02-28-08.pdf.
U.S. Environmental Protection Agency (EPA), 2010. Technical Support Document: Preparation of Emissions Inventories for the Version 4, 2005-based Platform, 73 pp., Office of Air Quality Planning and Standards, Air Quality Assessment Division. http://www.epa.gov/airquality/transport/pdfs/2005_emissions_tsd_07jul2010.pdf.